A major purpose of the Technical Information Center is to provide the broadest dissemination possible of information contained in DOE's Research and Development Reports to business, industry, the academic community, and federal, state and local governments.

Although a small portion of this report is not reproducible, it is being made available to expedite the availability of information on the research discussed herein.

Los Alamos National Laboratory is operated by the University of California for the United States Department of Energy under contract W-7405-ENG-36.

LA-UR--86-3863

DE87 005130

TITLE: SPECTROSCOPIC INVESTIGATION OF H^- AND D^- ION SOURCE PLASMAS

AUTHOR(S): H. Vernon Smith, Jr., Paul Allison, and Roderich Keller

SUBMITTED TO: Proceedings of the Fourth International Symposium on the Production and Neutralization of Negative Ions and Beams

Los Alamos Los Alamos National Laboratory
Los Alamos, New Mexico 87545

FORM NO 836 R4
ST NO 2629 5/81

MASTER

SPECTROSCOPIC INVESTIGATION OF H^- AND D^- ION SOURCE PLASMAS*

H. Vernon Smith, Jr., Paul Allison, and
Roderich Keller†, AT-2, MS H818
Los Alamos National Laboratory, Los Alamos, NM 87545

ABSTRACT

Several H I (Balmer), Cs I, Cs II, and Mo I lines emitted by the small-angle source and 4X source plasmas are studied. After correcting for Stark broadening, the H_α line width gives the H-atom temperature kT_{H0}. After correcting for Doppler broadening, the H_β and H_δ line widths give the electron density n_e. For pulsed operation of both sources, kT_{H0} is 1.5 to 2 eV and n_e is 1 to 2 x $10^{14}/cm^3$, with kT_{H0} and n_e scaling approximately with the square root of the discharge current. For the 4X source operated on D_2, kT_{D0} and n_e are near the values of kT_{H0} and n_e obtained for H_2 operation. Assuming that the H^-/D^- ion temperature equals the H/D-atom temperature, we deduce a lower limit to the H^-/D^- beam emittance.

INTRODUCTION

The Penning surface-plasma source (SPS) provides a bright H^- ion beam for accelerator applications.[1] Knowledge of the plasma parameters of this source may prove quite valuable in developing a theoretical model of it and in understanding its performance limits. In our initial study[2] of the plasma parameters of the Penning SPS discharge using quantitative optical spectroscopy, we looked only at the 4X source[3,4] discharge. The approximate plasma density, H-atom temperature, and electron temperature for only one set of discharge parameters for each of the three, pulsed-source plasma modes were determined. In this work we look in more detail at two of the 4X source discharge modes by varying the discharge parameters over a range of conditions, plus we study the small-angle source[5] (SAS) over a wide range of its operating parameters. We also take a brief look at the operation of the 4X source on deuterium. A preliminary report of the present work is given elsewhere.[6]

EXPERIMENTAL APPARATUS AND METHOD

Because the experimental method is discussed in Ref. 2, only a brief summary, including changes in the procedure, will be given here. A schematic of the experimental apparatus is shown in Fig. 1. The discharge light emitted from the source passes through a quartz vacuum window and is imaged with a lens onto the monochromator entrance slit. The monochromator slits are set for 0.01-nm full

*Work performed under the auspices of the U.S. Dept. of Energy and supported by the U.S. Army Strategic Defense Command.
†Permanent address: GSI, Darmstadt, West Germany.

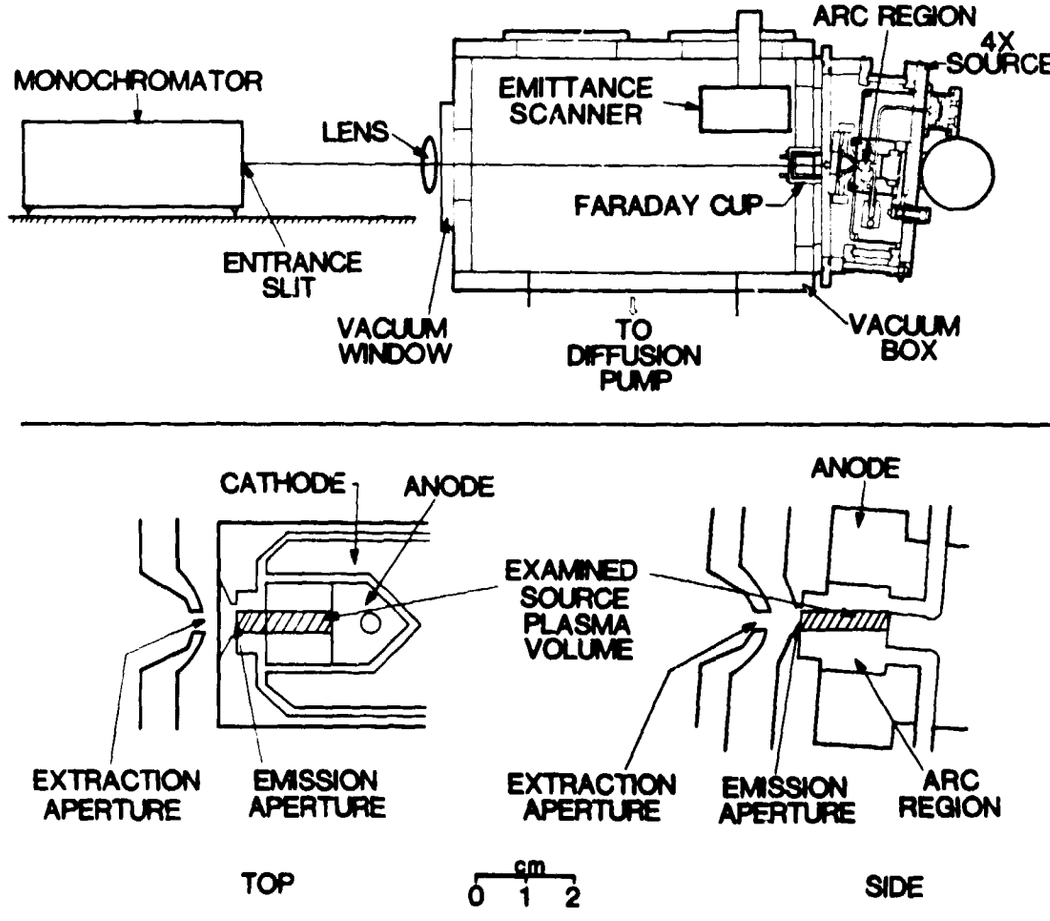

Fig. 1. Upper: experimental arrangement of the 4X source and the 1-m monochromator on the ion source test stand (not to scale). The distance from the emission aperture to the lens is 67 cm; to the monochromator, 107 cm.

Lower: horizontal (top) and vertical (side) sections of the 4X source plasma volume. Only a small portion (hatched area) of the arc region is examined with the monochromator.

half-width instrument broadening. The photomultiplier tube (PMT) current I_{PMT} is measured at a preselected time during the 1-ms-long discharge pulse by using a gated sample-and-hold circuit. This signal is then fed to the input of a strip-chart recorder. Because the strip-chart recorder and monochromator grating drive are driven at known constant speeds, the horizontal (time) axis is easily converted to wavelength. Sample recorded H_α, H_β, H_γ, and H_δ line shapes are shown in Fig. 2. The time required to record each curve in Fig. 2 was 1 min. The source pulsed-discharge repetition rate is 5 Hz; therefore, each curve is constructed from 300 discharge pulses.

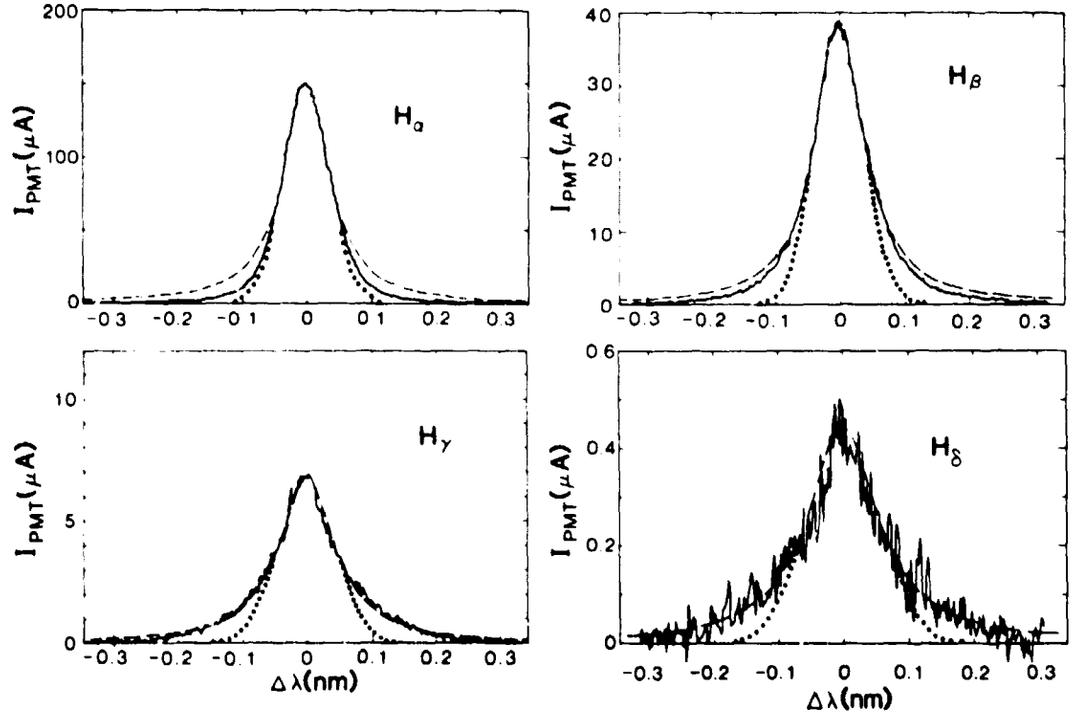

Fig. 2. H_α, H_β, H_γ, and H_δ Balmer line profiles recorded for a 152 A, Mode II discharge in the 4X source. The Lorentzian (dashed) and Gaussian (dotted) curves have the same half-widths as the measured profiles and are included for comparison purposes only.

The 4X source will operate in three distinct pulsed H_2 discharge modes (Table I of Ref. 4). Mode I has discharge voltage $V_D \approx 300$ V, with a 1500-G magnetic field and 2.2 Tl/s H_2 gas flow. At 29-keV extraction voltage, Mode I produces a maximum H^- beam current of 110 mA, having ±25% beam noise; Mode II, $V_D \approx 120$ V, 1500 G, 2.9 Tl/s, 120 mA of H^- at 29 keV with ±20% beam noise; and Mode III, $V_D \approx 500$ V, 700 G, 3.3 Tl/s, 70 mA of H^- at 29 keV with $\leq$±1% beam noise. We study two of these 4X source modes, Modes II and III, in this work. When the 4X source pulsed discharge is run on D_2 gas, it operates in Mode II. The SAS, with its fixed arc magnetic field, also operates in Mode II.

For each set of discharge conditions studied, we recorded the line profiles of the H_α, H_β, H_γ, and H_δ lines with 0.01-nm instrument resolution and the integral line intensities of several Cs I, Cs II, and Mo I lines (Table I of Ref. 2) with 0.05-nm instrument resolution. The electron temperature kT_e (determined from one ionization state of an element) is calculated from

$$kT_e=(E_j-E_i)/\ln[(A_j g_j \lambda_i I_i K_i)/(A_i g_i \lambda_j I_j K_j)] \qquad (1)$$

where E_i and E_j are the transition energies for two different lines; A the transition probabilities; g the statistical weights; λ the wavelengths; I the recorded integral intensities; and K the calibration factors. More details of this calculation are given in Ref. 2.

The measured hydrogen line profiles result from a convolution of Stark broadening, related to the electron density (ion-dynamical effects[7] further increase the Stark broadening of H_α); Doppler broadening, caused by the motion of radiating atoms; instrument profile; and the fine-structure splitting of the sublevels. For H_α profiles, a fine-structure correction curve is calculated following the procedure of Ref. 8, considering all seven sublevel positions. The fine-structure splitting is negligible for the other H-Balmer series profiles.

To separate Stark and Doppler broadening, a general tendency can be exploited: Doppler broadening scales proportionally to the wavelength of the observed line[9]; thus, H_α shows the largest Doppler broadening effect of the lines we examine. Stark broadening is larger for H_β and H_δ than for H_α and H_γ (Ref. 9). Therefore, H_α and H_γ should be better suited for atomic temperature determinations; H_β and H_δ, for electron density measurements. However, we find that H_γ has anomalous Lorentzian broadening (see below), so we do not use H_γ in any of our plasma-parameter determinations.

The actual unfolding procedure uses the tabulated Voigt function parameters.[10] Knowing the total width and the width of either a Gaussian or a Lorentzian profile, one can immediately look up the width of the other profile. Hydrogen Stark profiles have nearly Lorentzian shapes, whereas Doppler- and instrument-broadening effects produce Gaussian shapes. The instrument profile half-width is subtracted from the Doppler-broadening half-width by assuming they add quadratically. For the two 4X source deuterium measurements, we use the deuterium Doppler broadening, and we use the H_α fine-structure correction for D_α. For the D_α, D_β, and D_δ Stark-broadening corrections, we use the H_α (Ref. 11), H_β (Ref. 9), and H_δ (Ref. 9) values, respectively.

An iterative procedure is used to unfold the H-atom temperature and electron density from each set of H_α and H_δ measurements. Typically, four passes are required for kT_{H0} and n_e to converge. The kT_{H0} deduced in this manner is used to correct the H_β line for Doppler broadening, and the resulting H_β Stark broadening is used to obtain another value for n_e. Only the H_δ n_e values are used for the SAS (Fig. 6) because only in a few cases did we record the SAS H_β line shape. The rms deviation of the two values for n_e found from H_β and H_δ is 5%. Thus, we have good confidence in our values for n_e deduced from the hydrogen Balmer line shapes.

We have somewhat lower confidence in our kT_{H0} values because of the uncertainty in the theoretical knowledge of the Stark broadening of H_α. It is well known[7] that treating the ion motion in the static approximation leads to underestimating the Stark broadening of H_α for $n_e \sim 10^{14}/cm^3$ by about a factor of 3. To account for the ion motion (the "ion-dynamical effect"), Stehlé and Feautrier[11] use the impact approximation: we use their results in correcting our recorded H_α

line shapes for Stark broadening. However, Kelleher[12] has performed a calculation of ion dynamical broadening for H_α using a computer code that calculates the ion-generated perturbing fields using Monte Carlo techniques. For $kT_{H^+} = kT_e = 1$ eV and $n_e = 1 \times 10^{14}/cm^3$, Kelleher's prediction for the FWHM of H_α is 0.0089 nm, about 54% of Stehlé and Feautrier's 0.016 nm. If Kelleher's prediction is used, our values of kT_{H^0} deduced from the H_α line increase by 30%, the values of n_e deduced from H_β decrease by 15%, and the values of n_e deduced from H_δ decrease by 5%. Thus, the theoretical uncertainty in the Stark broadening of H_α causes ~30% uncertainty in our values for kT_{H^0} and ~10% uncertainty in our values for n_e. We note that the H-atom temperatures we report here (deduced from H_α) are for the n = 3 excited state. We assume that the H-atom temperatures for the ground state and n = 3, 4, and 6 excited states are identical. We do not use the recorded H_γ line shapes for any determination of the source plasma parameters because every H_γ line shape we record is almost entirely Lorentzian in shape (Fig. 2), despite its expected Doppler (Gaussian) shape. From Griem's tabulation of Stark widths,[9] H_γ is expected to have a very small Lorentzian half-width (about 0.01 nm). However, we observe H_γ has approximately 0.1-nm Lorentzian width. Evidently ion-dynamical effects are very important for H_γ. An investigation of this possibility is under way.[12] In our analysis, we assume local thermal equilibrium (LTE) and Maxwellian particle velocity distributions. These assumptions may not be valid.

RESULTS AND DISCUSSION

The deduced H-atom temperature vs discharge current for the 4X source is shown in Fig. 3; for the SAS, in Fig. 4. The electron density vs discharge current for the 4X source and SAS is shown in Figs. 5 and 6, respectively; the electron temperature vs discharge current, in Figs. 7 and 8. One of the most striking features of the results is the wide variation of the electron temperatures calculated from the Mo I, Cs I, Cs II, and H I integral line intensities. For the 4X source (Fig. 7), there is little variation of kT_e with I_d, and the average values for kT_e descend from 0.7 eV, for the Mo I results; to 0.6 eV, for Cs II; to 0.5 eV, for Cs I; to 0.2 eV, for H I. This general trend seems to hold true for the SAS as well (Fig. 8). This variation of kT_e with emitting species (hydrogen and cesium are purposely added to the source discharge, whereas the molybdenum comes from the sputtering of the molybdenum cathode material) probably indicates that the electron temperature distribution is not a simple Maxwellian.

The SAS has one primary mode of operation characterized by the discharge voltage being about 100 V--this corresponds most closely to Mode II for the 4X Source. The electron density vs I_d measurements for the SAS (Fig. 6) are all for this 100-V discharge mode. The SAS electron density varies approximately as the square-root of I_d. The same data for the 4X source, plotted in Fig. 5, are primarily for what we have termed Modes II and III. For completeness, on Fig. 5 we have included the four points we reported in Ref. 2. There appears to be a real difference between the plasma state of

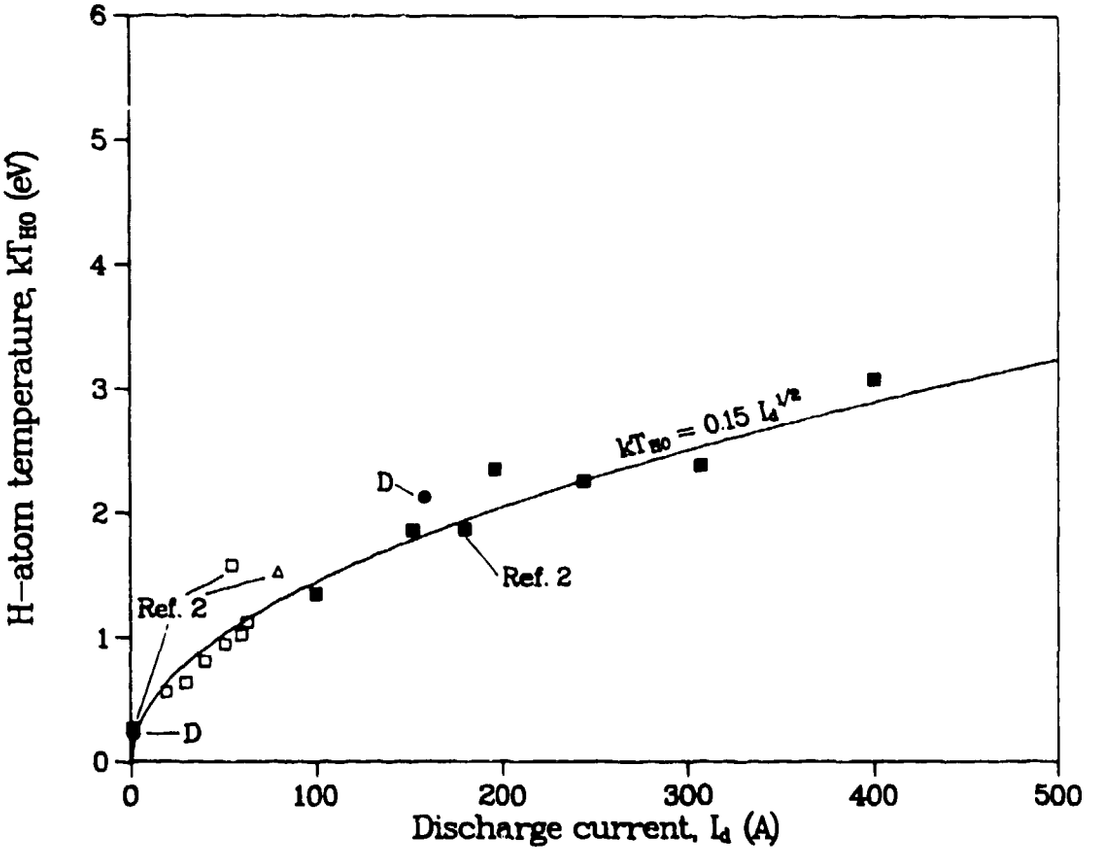

Fig. 3. H-atom temperature vs discharge current for the 4X source. The triangle is for Mode I, filled squares are for Mode II, and open squares are for Mode III. The filled circles are for a Mode II deuterium discharge. Four points from Ref. 2, corrected as discussed in the text, are included in this figure. The curve labeled $kT_{H0} = 0.15\ I_d^{1/2}$ is included to guide the eye.

Modes II and III. Mode III appears to have a nearly linear dependence of n_e on I_d, as one would naively expect. For Mode II, n_e appears to have about a $I_d^{1/2}$ dependence, which is not understood at present. We observe ±40% fluctuations on the discharge voltage and ±20% fluctuations on the H^- current from Mode II, but <±1% fluctuations of these parameters for Mode III. This leads us to speculate that plasma turbulence effects may exist in Mode II but not in Mode III (Ref. 2). These hypothetical plasma-turbulence effects may also cause anomalous plasma losses, hence the nonlinear dependence of n_e on I_d for Mode II. The $I_d^{1/2}$ dependence of n_e for the SAS suggests that plasma-turbulence effects may be important in that source also. Comparing the kT_e and kT_{H0} vs I_d curves for the SAS (Figs. 8 and 4, respectively), at the lowest I_d, $kT_e \gtrsim kT_{H0}$, as it is for most plasmas. However, for discharge currents $\geq$40 A, $kT_{H0} > kT_e$, difficult to understand unless our determination of kT_e

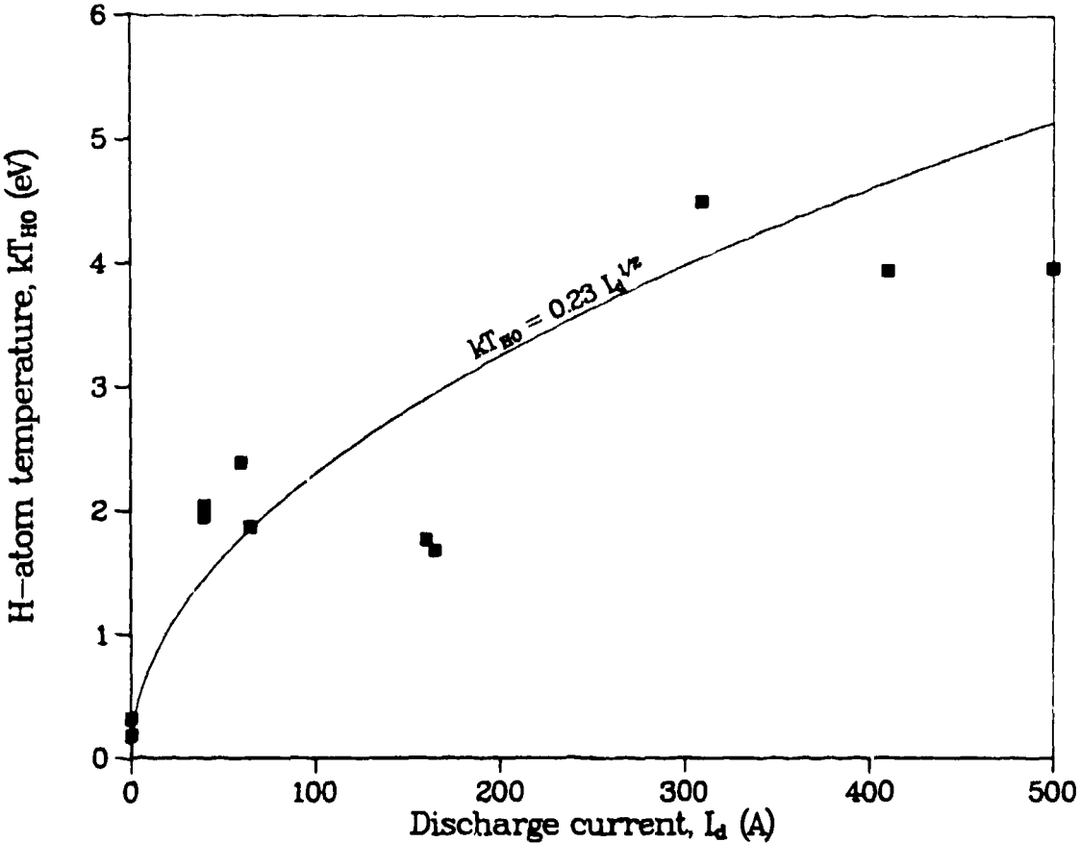

Fig. 4. H-atom temperature vs discharge current for the SAS. The curve labeled $kT_{H0} = 0.23\ I_d^{1/2}$ is included to guide the eye.

is inaccurate or there is anomalous heating of the atoms such as turbulence heating.

Despite the apparent difference in plasma state between Modes II and III, the 4X source H-atom temperature appears to depend as $I_d^{1/2}$ on the discharge current (Fig. 3), with the points from Modes II and III lying near the same curve. Use of the Stehlé correction[11] to the Stark broadening of H_α leads to the pulsed results in Ref. 2 being lowered an average of 28% for kT_{H0} and raised an average of 17% for n_e. The corrected kT_{H0} and n_e values are plotted on Figs. 3 and 5. The SAS kT_{H0} vs I_d curve (Fig. 4) also appears to follow approximately an $I_d^{1/2}$ dependence, but the scatter in the data is larger than that for the 4X source.

On Figs. 3 and 5 we have also included the results of two measurements on deuterium discharges in the 4X source. One point is for a low arc current, cw discharge (I_d = 1.3 A); the other for a high arc current, pulsed discharge (I_d = 158 A). The D-atom temperatures deduced from these two measurements are close to the H-atom temperature curve shown in Fig. 3. The maximum D^- current we have

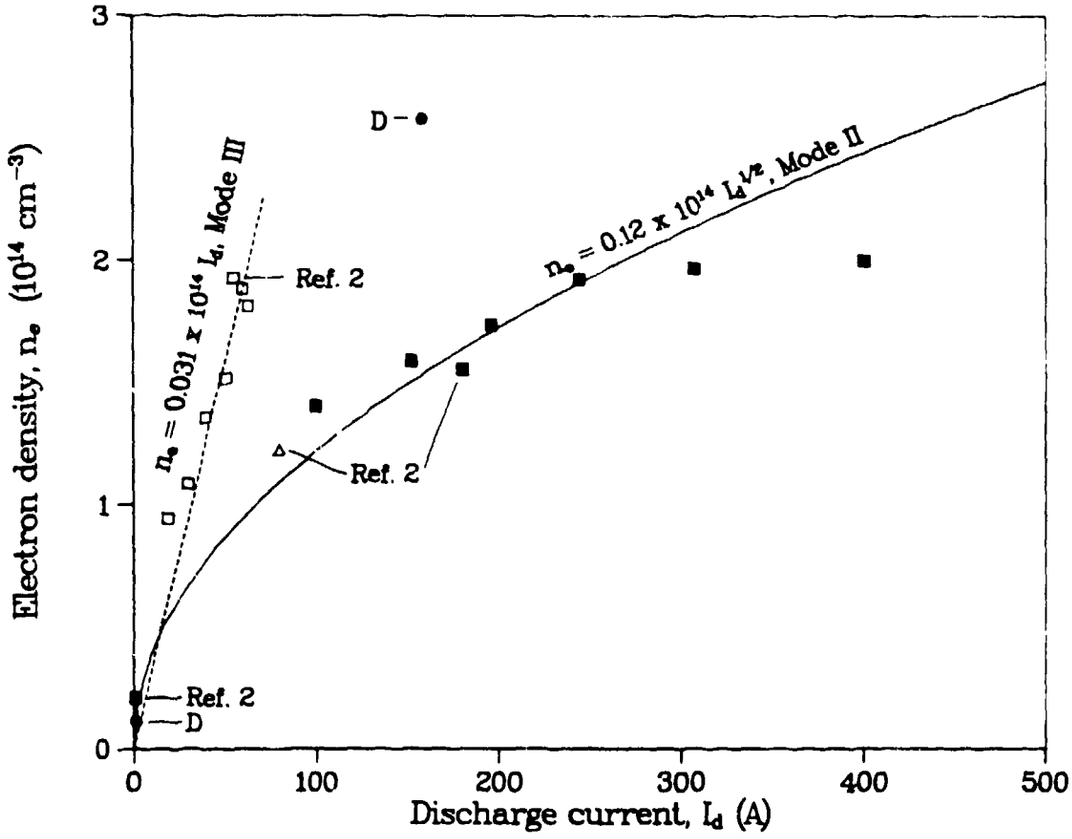

Fig. 5. Electron density vs discharge current for the 4X source. The legend for the points is given in the caption for Fig. 3. Four points from Ref. 2, corrected as discussed in the text, are included in this figure. The dashed straight line through the Mode III points, as well as the curve labeled $n_e = 0.12 \times 10^{14} I_d^{1/2}$, is included to guide the eye.

obtained from the 4X source at 29-keV extraction voltage is 55 mA for arc conditions that are not too different from those for which the 158-A deuterium spectroscopy measurements were made.

For pulsed operation of both the SAS and the 4X sources at their normal discharge currents of 150 A, the H-atom temperature is about 2 eV, considerably larger that the ~0.3 eV reported for the conventional duopigatron[13] and the bucket source.[13,14] Perhaps the relatively high H-atom temperature for the SAS and 4X sources is due to turbulence heating.

If the H^- ion temperature equilibrates with the H-atom temperature,[2] then we can compare the H^- ion temperature deduced from the spectroscopy measurements with that deduced from the SAS and 4X source[4] emittance measurements. To get the effective H^- temperature from the two-dimensional, rms emittance ε_{rms} we use[15]

$$\varepsilon_{rms} = R(kT_{H^-}/Mc^2)^{1/2}/2 \qquad (2)$$

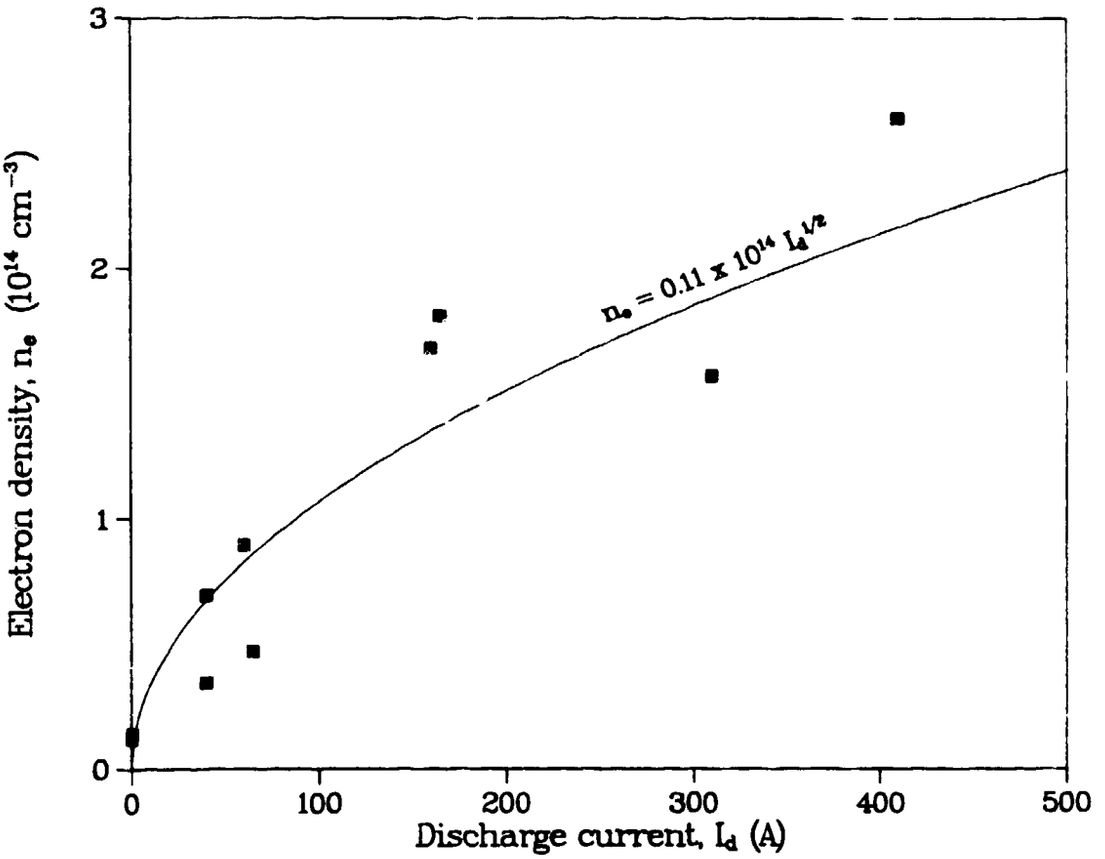

Fig. 6. Electron density vs discharge current for the SAS. The curve $n_e = 0.11 \times 10^{14} I_d^{1/2}$ is included to guide the eye.

where R is the emission aperture radius and M is the negative ion mass. The H^-/D^- current, current density, and ion temperature values are given in Table I. We note that the kT_{H^-} values deduced from the spectroscopy measurements are considerably below the values deduced from the emittance (phase-space) measurements. This difference can arise from either the H^- ion temperature being much larger than the H-atom temperature (nonequilibrium, despite our estimate) or from effects other than temperature contributing to ε_{rms}. These effects can include aberrations in the extraction system, perveance fluctuations in the extraction gap, dispersion of the H^- ions in the source magnetic field, and nonlinear space-charge compensation effects in the H^- beam transport. We think that the first two effects are likely to be much more important than the latter two.[2,4] Using the spectroscopy value for kT in Eq. (2), we determine a lower limit to ε_{rms} for the 4X source and the SAS. These limits are 0.0044 and 0.0093 π•cm•mrad respectively, considerably below our lowest measured ε_{rms} for these sources, 0.011 and 0.018 π•cm•mrad.

Finally, although we have not made emittance measurements of the D^- beam from the 4X source, from the spectroscopy measurements we deduce that kT_{H^0} and kT_{D^0} are approximately equal. If $kT_{H^0} = kT_{H^-}$ and $kT_{D^0} = kT_{D^-}$, then we would expect ε_{rms} for D^- to be ~0.7 ε_{rms} for H^-.

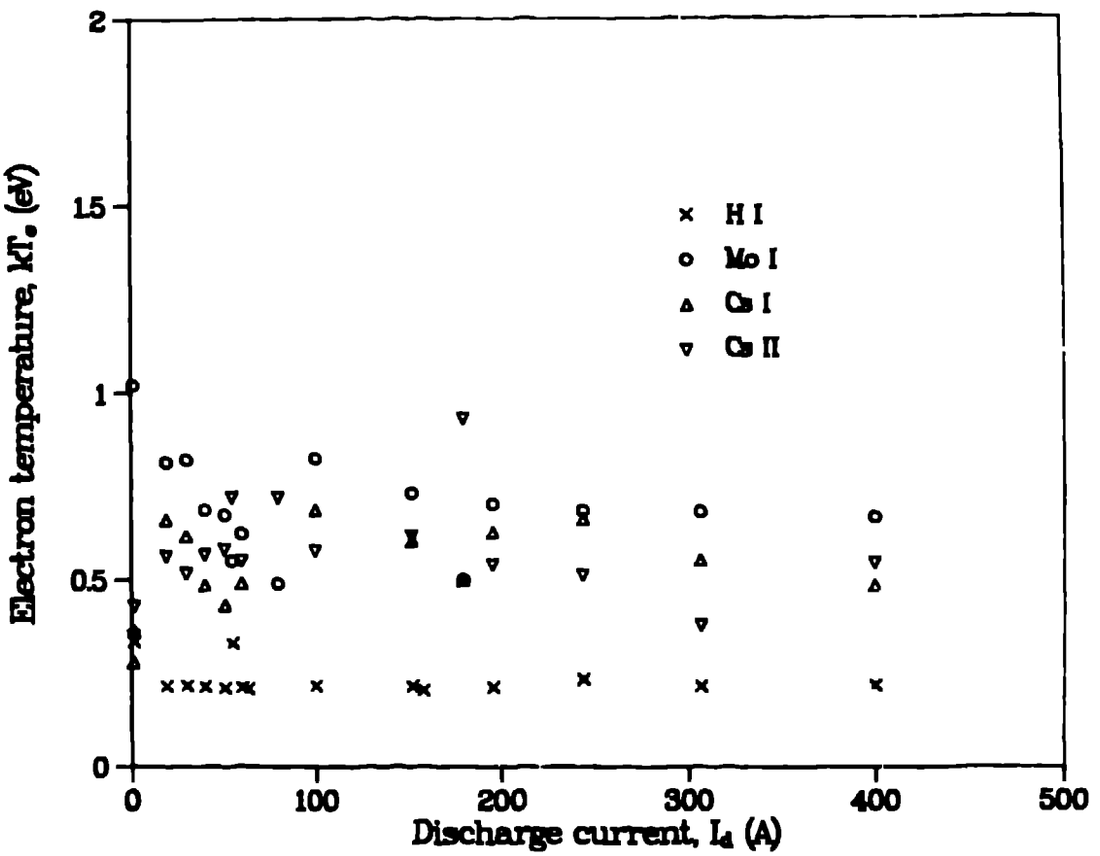

Fig. 7. Electron temperature vs discharge current for the 4X source. The legend for the points is given on the figure.

TABLE I Current, current density, and ion temperature values

Ion	Source (Discharge Mode)	I_- (mA)	j_- (mA/cm^2)	kT_H- Spectroscopy Value[a] (eV)	kT_H- Phase-Space Value[b] (eV)
H^-	4X (I)	110	480	1.5	15
H^-	4X (II)	100	437	1.9	25
D^-	4X (II)	50	218	2.1	--
H^-	4X (III)	67	293	1.0	6.2
H^-	SAS (II)	140	2800	2.0	6.6

[a] Assumes $kT_H{}^0$ equals $kT_H{}^-$.

[b] Calculated from $kT = 4\, c_{rms}{}^2 Mc^2/R^2$ for 4X source and $kT = 3\, c_{rms}{}^2 Mc^2/a^2$ for the SAS (Ref. 15).

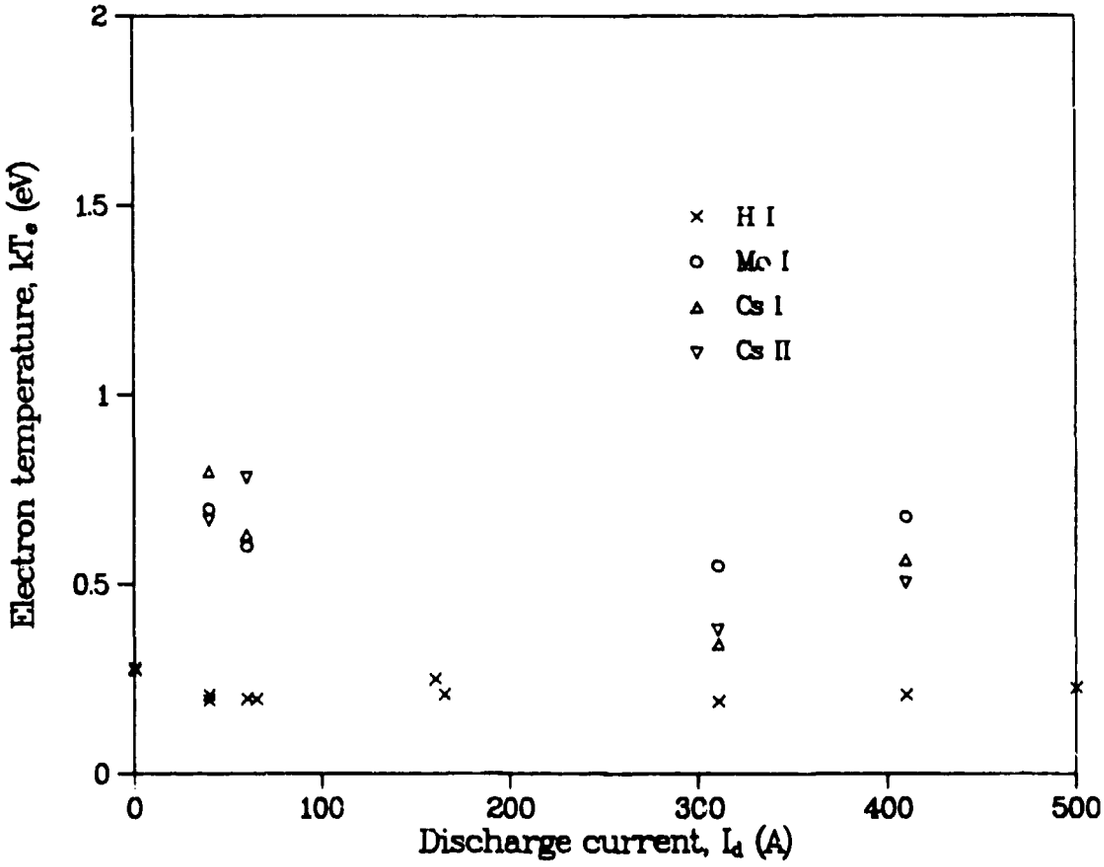

Fig. 8. Electron temperature vs discharge current for the SAS. The legend for the points is given on the figure.

CONCLUSIONS

For pulsed operation of the 4X and small-angle sources, kT_{H^0} is 1.5 to 2 eV and n_e is 1 to 2 x 10^{14} cm^{-3}. If kT_{H^0} gives a true indication of the H^- ion temperature in the source plasma, then a factor of 1.8 to 3.6 reduction in the H^- beam emittance may be possible.

REFERENCES

1. G.E. Derevyankin and V.G. Dudnikov, "Production of High Brightness H^- Beams in Surface-Plasma Sources," AIP Conf. Proc. No. 111, AIP, New York, 376 (1984).

2. R. Keller and H.V. Smith, Jr., IEEE Trans. Nucl. Sci. 32, (5) 1736 (1985).

3. H.V. Smith, Jr., P. Allison, and J.D. Sherman, "A Scaled, Circular-Emitter Penning SPS for Intense H^- Beams," AIP Conf. Proc. No. 111, AIP, New York, 458 (1984).

4. H.V. Smith, Jr., P. Allison, and J.D. Sherman, IEEE Trans. Nucl. Sci. 32, (5) 1797 (1985).

5. P. Allison and J.D. Sherman, "Operating Experience With a 100-keV, 100-mA H^- Injector," AIP Conf. Proc. No. 111, AIP, New York, 511 (1984).

6. R. Keller, H.V. Smith, Jr., and P. Allison, Bull. Am. Phys. Soc. 30, 1608 (1985).

7. J. Seidel, in Spectral Line Shapes, edited by B. Wende (de Gruyter, New York, 1981), p. 3.

8. M.W. Grossman, "H^- Ion Source Diagnostics," Proc. of Symp. on the Production and Neutralization of Negative Hydrogen Ions and Beams, Brookhaven National Laboratory report BNL-50727, 105 (1977).

9. H.R. Griem, Spectral Line Broadening by Plasmas, (Academic Press, New York, 1974)

10. G. Traving, in Plasma Diagnostics, ed. W. Lochte-Holtgreven, (North Holland, Amsterdam, 1968), Chap. 2.

11. C. Stehlé and N. Feautrier, J. Phys. B: At. Mol. Phys. 17, 1477 (1984).

12. D.E. Kelleher, National Bureau of Standards, Washington, D.C., 20234. Private communication.

13. D.H. McNeill and J. Kim, Phys. Rev. A 25, 2152 (1982).

14. M. Pealat, J-P.E. Taran, M. Bacal, and F. Hillion, J. Chem. Phys. 82, 4943 (1985).

15. P. Allison, J.D. Sherman, and H.V. Smith, Jr., "Comparison of Measured Emittance of an H^- Ion Beam with a Simple Theory," Los Alamos National Laboratory report LA-8808-MS (June 1981).